

## Evidence of a Sponge-to-Lamellar Phase Transition under Shear by X-Ray Scattering Experiments in a Couette Cell

H. F. Mahjoub,<sup>1</sup> C. Bourgaux,<sup>1,2</sup> P. Sergot,<sup>1,3</sup> and M. Kleman<sup>1</sup>

<sup>1</sup>LMCP Université Pierre et Marie Curie, case 115, 4 place Jussieu, F-75252 Paris Cédex 05, France

<sup>2</sup>LURE, Centre Universitaire, F-91405 Orsay Cedex, France

<sup>3</sup>ESPCI 10 rue Vauquelin, F-75005, Paris, France

(Received 10 July 1997; revised manuscript received 3 November 1997)

The  $L_3$  sponge phase under shear in a Couette cell is totally transformed to a lamellar phase  $L_{\alpha^*}$  above some critical shear rate  $\dot{\gamma}_c$ . *In situ* x-ray scattering and simultaneous light microscopy observations show that the first nuclei of the  $L_{\alpha^*}$  phase appear at a low critical shear rate  $\dot{\gamma}_a$  and that the orientation of the lamellae in the  $L_{\alpha^*}$  phase tilts over from a so-called “a” orientation to a “c” orientation at  $\dot{\gamma}_c$ . In the regime with two phases  $\dot{\gamma}_a$  and  $\dot{\gamma}_c$ , the phases are in an epitaxial relationship immediately after the shear is removed. [S0031-9007(98)07037-9]

PACS numbers: 61.25.-f, 47.15.-x, 61.10.Eq

We report on a series of experiments relating to the structural modifications which affect the symmetric sponge phase  $L_3$  under shear. This phase is an optically isotropic liquid, made of a (unique) 3D random multiply connected bilayer of surfactant molecules, dividing the solvent into two equivalent subvolumes [1]. The system under study consists of a quaternary ammonium surfactant: cetylpyridinium chloride (CpCl, H<sub>2</sub>O content 1 mol/mol), a cosurfactant: hexanol, and brine (1 wt % NaCl) as a solvent, in the solvent weight fraction range  $0.85 < \phi_s < 0.95$ .

Transitions between  $L_3$  and  $L_{\alpha}$  phases at equilibrium have already been studied as a function of temperature [2], salt concentration [3], or cosurfactant/surfactant ratio [4]. In this paper we confirm by x-ray scattering former rheoptical measurements [5] which showed that shearing is also capable of inducing a sponge-to-lamellar transition; this result agrees with Cates and Milner’s theory [6]. Yamamoto and Tanaka [7] have also obtained evidence of  $L_3$  to  $L_{\alpha}$  transition under oscillatory shear flow (see also [8]). Recently this transition was numerically simulated by Emerton *et al.* [9]. Diat and Roux [10] found, for a quaternary  $L_3$  system, a regime of shear birefringence above some threshold, but their results leave the question of the transition an open issue. See Plano *et al.* [11] for similar conclusions. On the other hand Bruinsma and Rabin [12] claim that the  $L_{\alpha}$  phase could be unstable with respect to the  $L_3$  phase by enhancement of short wavelength concentration fluctuations under shear.

The present results originate from small-angle x-ray scattering data collected during shear and from optical observations just after shear and during relaxation. We do not know of any previous optical observations of textures coupled to a phase transition under shear. X-ray scattering experiments were conducted at the D24 beam line of the LURE-DCI synchrotron radiation facility. A Couette cell (gap = 0.5 or 1 mm) has been specially designed to carry out simultaneously *in situ* x-ray scattering and optical microscopic observations. The x-ray beam can be

chosen parallel either to the shear gradient (radial geometry) or to the velocity (tangential geometry). A light polarizing microscope is fitted to this cell perpendicular to the x-ray beam, in the horizontal plane. Since the samples are so thick, we have no direct evidence of the nature of the anchoring but there are all reasons to believe that it is homeotropic as usual in lyotropic systems. The recording time of the spectra is 20–30 s in the radial geometry and 300–600 s in the tangential one. The typical rotation period of the Couette cell is never larger than 15 s in all experiments.

One distinguishes experimentally several regimes: at low shear rates, the  $L_3$  phase keeps its structural properties mostly unchanged, whereas, at higher ones, it is deformed in a fundamental way. Scattering patterns show that the first nuclei of lamellar phase select an “a” orientation (i.e., layers normal orient perpendicularly to both the shear and the shear gradient [13,14]); then the fraction of material turned to a lamellar phase increases, eventually leading to the complete transformation of the sponge phase to a  $L_{\alpha^*}$  phase (here and below the asterisk denotes a *sheared* lamellar steady state) with layers in the “c” orientation (i.e., layers orient perpendicularly to the velocity gradient [10,13]). Rheoptical data make these dynamical aspects [5,15] more precise.

In Table I,  $d_3$  is the characteristic length of the  $L_3$  phase,  $\eta$  is the dynamical viscosity,  $d_{\alpha^*}$  the repeat distance of the  $L_{\alpha^*}$  phase,  $\dot{\gamma}_a$  ( $\dot{\gamma}_c$ ) is the threshold shear rate at which the first nuclei of  $L_{\alpha^*}$  appear with an a orientation (the tilt to a c orientation occurs). Most of these material constants relate to two compositions, sample A:  $\phi_s = 0.85$ ,  $h/c = 1.12$ , sample B:  $\phi_s = 0.90$ ,  $h/c = 1.15$ . Here  $h/c$  is the weight ratio of the cosurfactant ( $h$ ) and the surfactant ( $c$ ) in the bilayers.

*Low shear rates*,  $0 < \dot{\gamma} < \dot{\gamma}_a$ .—X-ray scattering shows a broad peak at  $q_3 = 2\pi/d_3$  [curve 1, Fig. 1(a)];  $d_3$  is the characteristic size of passages of the random structure and does not differ significantly from its rest value.

TABLE I. Characteristic values of our samples.

	$h/c$ (wt ratio)	$\phi_s$ (wt fraction)	$\eta$ (cp) $\dot{\gamma} = 20 \text{ s}^{-1}$	$d_3$ (nm) at rest	$d_{\alpha^*}$ (nm) curve 2	$d_{\alpha^*}$ (nm) curve 3	$d_{\alpha^*}$ (nm) curve 4	$\dot{\gamma}_a$ ( $\text{s}^{-1}$ )	$\dot{\gamma}_c$ ( $\text{s}^{-1}$ )
A	1.12	0.85	7.4	22	16.5	16.8	18	$\sim 25$	$\sim 43$
B	1.15	0.90	5.7	33	23.7	24.0	26.1	$\sim 12$	$\sim 20$

*Intermediate shear rates,  $\dot{\gamma}_a < \dot{\gamma} < \dot{\gamma}_c$ .*—A Bragg peak appears at  $q > q_3$  [curve 2, Fig. 1(a)] proving the existence of regular stacks of  $L_{\alpha^*}$  lamellae. With increasing time of shearing and/or shear rates, this narrow peak continues to grow at the expense of the  $L_3$  phase until state 3 [curve 3, Fig. 1(a)]. At the same time the distance between layers slightly increases. The sample is biphasic: in state 3 the amount of remaining  $L_3$  phase is about 25%–30%. The content of the  $L_3$  phase was evaluated by fitting the original  $L_3$  curve to intermediate scattering profiles. The orientation of the layers may

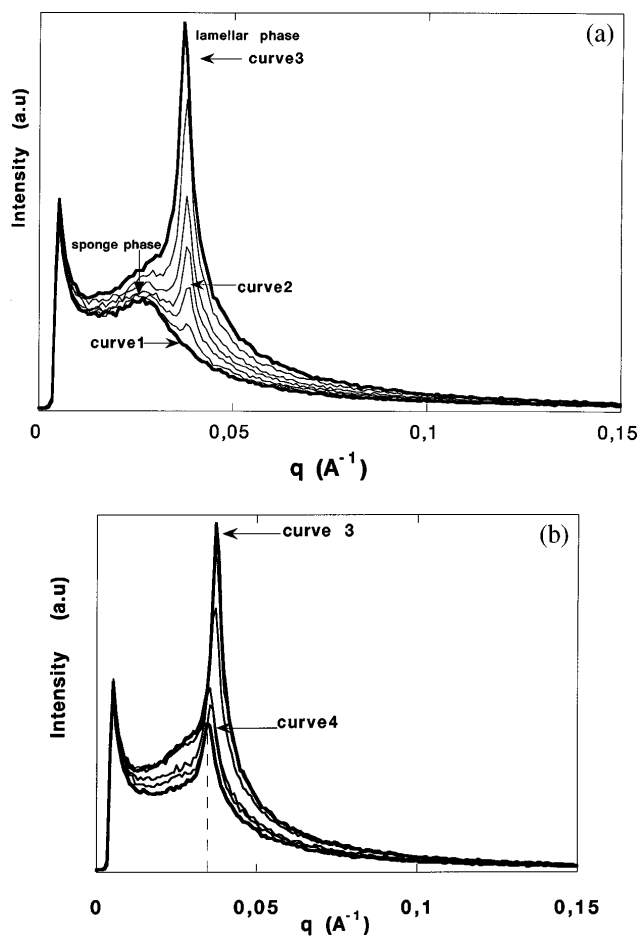


FIG. 1. Sample A: (a) X-ray spectra in radial geometry at different shear rates; curve 1 (state 1): sponge phase at  $\dot{\gamma} = 15 \text{ s}^{-1}$ ; curve 2 (state 2): biphasic  $L_3/L_{\alpha^*}$  domain obtained after  $9 \times 30 \text{ s}$  at  $\dot{\gamma} = 30 \text{ s}^{-1}$ ; curve 3 (state 3): obtained after shearing  $28 \times 30 \text{ s}$  at  $\dot{\gamma} = 40 \text{ s}^{-1}$ . (b) Decrease of the scattered intensity in radial geometry during the change of orientation; state 4 is reached from state 3 after  $400 \text{ s}$  shear at  $\dot{\gamma} = 50 \text{ s}^{-1}$ .

be probed by x-ray scattering in the  $(z, \nu)$  plane (radial geometry) and in the  $(z, \nabla \nu)$  plane (tangential geometry). In the  $(z, \nu)$  plane the scattering patterns exhibit two spots along the  $z$  direction, coexisting at low  $\dot{\gamma}$  or  $t$  with the isotropic scattering ring arising from the remaining  $L_3$  phase [Fig. 2(a), state 3]. In the  $(z, \nabla \nu)$  plane the lamellar spots are curved into arcs [Fig. 2(b), state 3]. These observations show that lamellae which form are mainly in the  $a$  orientation.

Thermally excited elastic fluctuations of SmA layers yield a scattered intensity power law [16]:

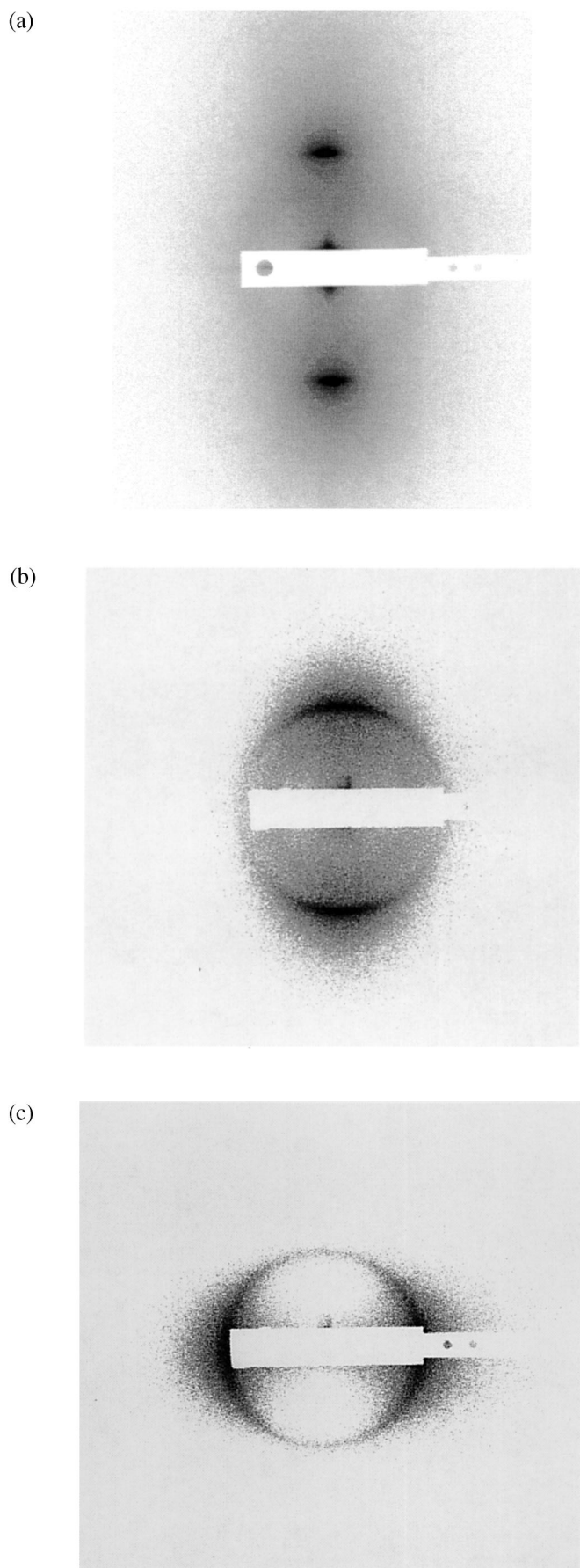
$$I(0, 0, q_z) \sim |q_z - q_0|^{-2+\chi} \quad (1)$$

with

$$\chi = \frac{q_0^2 k_B T}{8\pi \sqrt{BK}}, \quad (2)$$

where  $B$  and  $K$  are the bulk moduli for layer compression and layer curvature ( $K \sim 2 \times 10^{-12} \text{ J/m}$ ,  $\bar{B} \sim 6 \times 10^2 \text{ J/m}^3$  for  $d_\alpha \sim 20 \text{ nm}$ , and  $\bar{B}$  is the bulk modulus for layer compression at constant potential which can be measured experimentally while  $B$  cannot). We find  $\chi \cong 1.05$  [close to state 3 in Fig. 1(a)]. This value is close to  $\chi(d) = 1.33(1 - \delta/d)2$  predicted in [17] and agrees well with measurements in other membranar systems ( $\delta$  is the thickness of the membrane). Higher order Bragg peaks are not observed, since large undulation fluctuations destroy the long range order when  $\chi \neq 0$  [18]. When shear is ceased after reaching a state between 2 and 3, lamellar nuclei melt and transform back into  $L_3$ , and the initial  $L_3$  scattering profile is progressively recovered; intriguingly the system goes through the same intermediate states as during the shear rate increase process. The integrated intensity relaxes in an exponential way— $t_{\text{rel}} \cong 100 \text{ s}$  (state 3, sample A)—in agreement with optical observations of  $L_{\alpha^*}$  nuclei conducted immediately after shear ceasing. Figure 3(a) (after ceasing shear at  $\dot{\gamma} = 25 \text{ s}^{-1}$ ) shows  $L_{\alpha^*}$  nuclei slowly shrinking in the  $L_3$  matrix: their shape is similar to that observed in the biphasic domain  $L_\alpha$ - $L_3$  at rest, an indication that the  $L_\alpha$  layers make a constant angle with the interface [19]; this has been interpreted in terms of epitaxy between  $L_\alpha$ , and  $L_3$ , i.e., matching of the characteristic lengths  $d_3$  and  $d_\alpha$  at the interface. At  $\dot{\gamma} = 30 \text{ s}^{-1}$ —a state close to 3—we observe a dense population of lamellar nuclei; at higher  $\dot{\gamma}$  (i.e.,  $\dot{\gamma} = 40 \text{ s}^{-1}$ ) the number of nuclei increases while their size decreases (from  $\sim 50 \mu\text{m}$  to  $\sim 20\text{--}30 \mu\text{m}$ ).

*High shear rates,  $\dot{\gamma} > \dot{\gamma}_c$ .*—Above some critical threshold  $\dot{\gamma}_c$  ([5], Table I),  $L_3$  completely transforms to



a  $L_{\alpha^*}$  phase: the  $L_3$  bump disappears. During this last step, the  $L_{\alpha^*}$  Bragg peak shifts to smaller values and its intensity, measured along the  $z$  direction, decreases [state 4, Fig. 1(b)], suggesting a change of orientation of the lamellae. This is confirmed by the scattering pattern in tangential geometry: it is made of two strong arcs along  $\nabla v$  with a weak tail extending along the  $z$  axis [Fig. 2(c)]; thus the layers orientation, previously  $a$ , is now mostly parallel to the walls of the cell ( $c$  orientation). These results are confirmed by observations between crossed polars: just after state 3, the field of view is filled with oily streaks along the flow [20]. When we stop shearing at state 3 or just after, the  $L_3$  nuclei which grows in the  $L_{\alpha^*}$  matrix are elongated parallel to the  $L_{\alpha^*}$  bilayers and show up faceting [Fig. 3(b)]. This relaxation process requires long durations: we recover 30%–40% of the sponge phase after  $\sim 3$ –4 hr. At values higher than  $\dot{\gamma}_c$ , we obtain a homogeneous dark field between crossed polars, defects are eliminated, and it seems that the lamellae are “stabilized”: relaxation to the  $L_3$  phase is not observed, and only confocal domains of the first species [20] appear.

We believe that, in the coexistence region, the  $L_{\alpha^*}$  nuclei are not in strict epitaxy with the  $L_3$  matrix. Indeed, we observe lamellar nuclei with a spiral logarithmic shape only a few seconds after ceasing shear, during which some reorganization takes place [Fig. 3(a)]. The size of  $L_{\alpha^*}$  nuclei decreases and becomes rather monodisperse near state 3 while the number of nuclei increases. An estimation of their size, balancing nucleus free energy, and dissipation yields either  $R \propto \sqrt{\kappa/\eta d_{\alpha^*} \dot{\gamma}}$  if elastic terms are predominant or  $R \propto \sigma/\eta \dot{\gamma}$  if surface terms. For sample A ( $\kappa \approx kT$ ,  $\dot{\gamma} \approx 50 \text{ s}^{-1}$ ,  $\sigma \approx 10^{-6} \text{ J/m}^2$ —from the estimation in [21]), one gets  $R \approx 1 \mu\text{m}$  in the first case and  $R \approx 50$ – $100 \mu\text{m}$  in the second case. The order of magnitude of the size nuclei indicates predominance of the surface terms.

The increase in periodicity  $d_{\alpha^*}$  under shear from state 3 to state 4 might result from a difference in composition of the  $L_{\alpha^*}$  and  $L_3$  phases in contact, as observed for the biphasic  $L_3/L_{\alpha}$  at rest. Note also that the lamellar phase  $L_{\alpha}$  close to the  $L_3$  boundary [22,23] preserves some characteristics of the sponge phase, in particular, a high density of passages, and it would be tempting to think that passages should decrease in size and thereby tend to close. Upon ceasing shear in state 4, there is no further variation of  $d_{\alpha^*}$ . It would be interesting to correlate these results with previous viscosity measurements [5] showing that the viscosity  $\eta$  of the sponge phase remains almost constant throughout the  $L_3/L_{\alpha^*}$  phase transition and, indeed, reaches a value close to  $\eta(L_{\alpha})$  for a  $L_{\alpha}$

FIG. 2. Sample A, bidimensional scattering patterns under shear: (a) State 3, radial geometry; (b) state 3, tangential geometry; (c) state 4, tangential geometry.

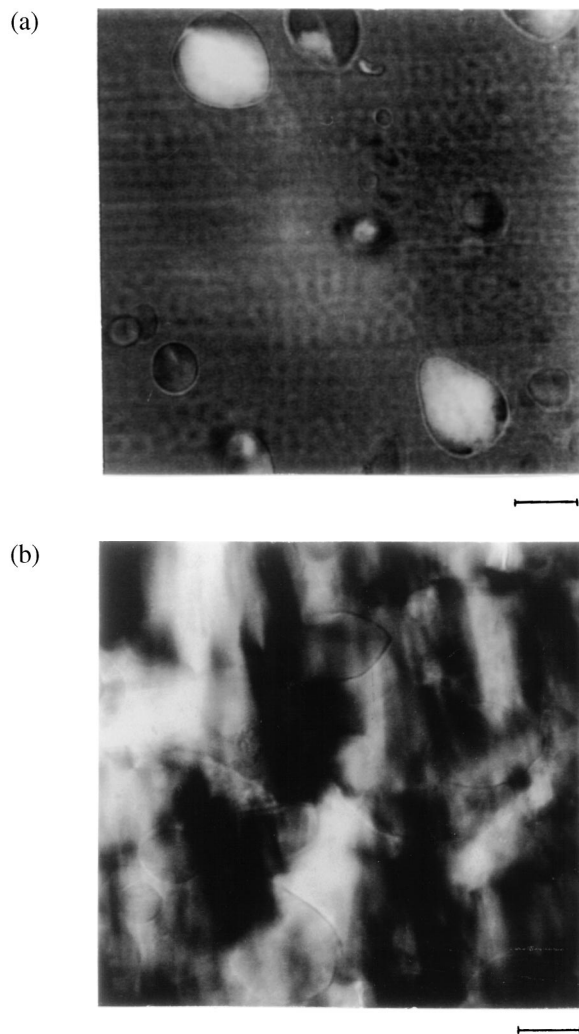


FIG. 3. Sample A, light microscopy (crossed polars) (a) between states 2 and 3:  $L_{\alpha^*}$  domains in epitaxy with matrix  $L_3$ ; (b) between states 3 and 4: focal conic domains perpendicular to the lamellae, note the angular orientated shape of the  $L_3$  droplet indicating epitaxy.

close to the  $L_3$  composition. However, we have no model describing viscosity as a function of passages' density.

Hereafter we try to describe qualitatively the orientational  $a$  to  $c$  transition; the shape of the scattering arcs of state 3 in radial [Fig. 2(a)] and tangential geometries [Figs. 2(b) and 2(c)] suggest an oblate cylindrical stacking of bilayers, elongated along the velocity. The axes of these objects coincide with the flow direction so that to first obtain lamellae in the  $a$  orientation, then lamellae parallel to the  $c$  orientation, it suffices to rotate around this axis.

On the whole, our results agree with [6] for the appearance of a lamellar phase with  $a$  orientation; they can also

be compared with those of [24] whose authors have found two distinct lamellae orientations in dynamically sheared diblock copolymer melts (see also [25]). A more detailed discussion will appear in a future work [26].

We thank Professor J.F. Tassin for valuable discussions, and Professor K. McGrath for useful comments.

- 
- [1] M.E. Cates, D. Roux, D. Andelman, S.T. Milner, and S.A. Safran, *Europhys. Lett.* **5**, 733 (1988).
  - [2] Y. Nastichin, E. Lambert, and P. Boltenhagen, *C. R. Acad. Sci. Paris* **321**, 205 (1995).
  - [3] C. A. Miller and O. Ghosh, *Langmuir* **2**, 321 (1986).
  - [4] G. Porte, J. Marignan, P. Bassereau, and R. May, *J. Phys. (Paris)* **49**, 511 (1988).
  - [5] H.F. Mahjoub, K.M. McGrath, and M. Kleman, *Langmuir* **12**, 3131 (1996).
  - [6] M.E. Cates and S.T. Milner, *Phys. Rev. Lett.* **62**, 1356 (1989).
  - [7] J. Yamamoto and H. Tanaka, *Phys. Rev. Lett.* **77**, 4390 (1996).
  - [8] H. Hoffmann, S. Hoffmann, A. Rauscher, and J. Kalus, *Prog. Colloid. Polym. Sci.* **84**, 24 (1991).
  - [9] A. Emerton, F. Weig, P. Coveney, and B. Boghian, *J. Phys. Condens. Matter* **9**, 8893 (1997).
  - [10] O. Diat and D. Roux, *Langmuir* **11**, 1392 (1995).
  - [11] R.J. Plano, C.R. Safinya, E.B. Sirota, and L.J. Wenzel, *Rev. Sci. Instrum.* **4**, 1309 (1993).
  - [12] R.F. Bruinsma and I. Rabin, *Phys. Rev. A* **45**, 994 (1992).
  - [13] M. Goulian and S.T. Milner, *Phys. Rev. Lett.* **74**, 1775 (1995).
  - [14] S. Ramaswamy, *Phys. Rev. Lett.* **69**, 112 (1992).
  - [15] H.F. Mahjoub, J.F. Tassin, and M. Kleman (to be published).
  - [16] A. Caillé, *C. R. Acad. Sci. Paris* **B274**, 891 (1972).
  - [17] W. Helfrich, *Z. Naturforsch. A* **33**, 305 (1987).
  - [18] F. Nallet, R. Laversanne, and D. Roux, *J. Phys. II (France)* **3**, 487 (1993).
  - [19] C. Quillet, C. Blanc, and M. Kleman, *Phys. Rev. Lett.* **77**, 522 (1996).
  - [20] P. Boltenhagen, M. Kléman, and O. Lavrentovich, in *Soft Order in Physical Systems*, edited by Y Rabin and R. Bruinsma (Plenum Press, New York, 1994), p. 5.
  - [21] O.D. Lavrentovich, C. Quillet, and M. Kleman, *J. Phys. B* **101**, 421 (1997).
  - [22] R. Strey, W. Jahn, G. Porte, and P. Bassereau, *Langmuir* **6**, 1635 (1990).
  - [23] P. Boltenhagen, M. Kleman, and O. Lavrentovich, *J. Phys. II (France)* **4**, 1439 (1994).
  - [24] K. A. Koppy *et al.*, *J. Phys. II (France)* **2**, 1641 (1992).
  - [25] Y. Zhang and U. Wiesner, *J. Chem. Phys.* (to be published).
  - [26] H. Mahjoub, C. Bourgaux, J.F. Tassin, P. Sergot, and M. Kleman (to be published).